Morphology of the Undersurface of the Anterolateral Acromion and Its Relationship to Surrounding Structures

Yusuke Ueda,*† MD, Akimoto Nimura,‡§ MD, PhD, Keisuke Matsuki,† MD, PhD, Kumiko Yamaguchi,* MD, PhD, Hiroyuki Sugaya,‖ MD, PhD, and Keiichi Akita,* MD, PhD

Investigation performed at the Department of Clinical Anatomy, Graduate School of Medical and Dental Science, Tokyo Medical and Dental University, Tokyo, Japan

Background: A better understanding of the morphology underneath the acromion is needed to prevent complications after arthroscopic subacromial decompression. The precise correlations between the morphologic features underneath the acromion and the surrounding structures including the attachment of the coracoacromial ligament (CAL) and the origin of the deltoid middle head have not yet been determined in the absence of artifacts on the bony surface caused by dissection techniques. Moreover, anatomic findings in previous studies using only older-aged cadavers or dried bones may not reflect the morphologic features of younger and healthy specimens.

Purpose: To characterize the anterolateral structures morphologically in the inferior aspect of the acromion, assess the relationships of these structures with surrounding structures without dissection artifacts on the bony surface, and verify the cadaveric data in the asymptomatic shoulders of living middle-aged patients.

Study Design: Descriptive laboratory study.

Methods: We initially analyzed the relationship between the morphology of the anterolateral structures and surrounding structures in 18 cadaveric shoulders (mean age, 81.8 years), 15 of which were subjected to macroscopic investigation of the CAL attachment and 3-dimensional micro—computed tomography investigation with radiopaque markers and 3 of which were subjected to histologic examination. We also analyzed the morphology underneath the anterolateral acromion in 24 asymptomatic shoulders of middle-aged patients (mean age, 54.8 years) to verify the cadaveric data. In both the cadaveric shoulders and the asymptomatic shoulders of live patients, the long axis, width, and height of the anterolateral prominence were measured by use of 3-dimensional CT imaging.

Results: In cadavers, the anterolateral prominence underneath the acromion corresponded to the attachment of the CAL. Histologic evaluation revealed that the CAL was continuous to the deep layer of the deltoid middle head in the lateral acromion. The study in asymptomatic shoulders of middle-aged patients revealed bony prominences similar to those observed in cadavers.

Conclusion: The anterolateral prominence, which corresponds to the attachment of the CAL below the acromion, may be a native structure below the acromion. Moreover, the CAL is continuous to the deep layer of the deltoid middle head in the lateral acromion.

Keywords: shoulder; acromion; anterolateral prominence; coracoacromial ligament; deltoid muscle; computed tomography; anatomy

Previous reports have described relationships between protraction of the acromial spur and impingement syndrome or rotator cuff tears (RCTs).[10,21-23] Arthroscopic subacromial decompression (ASD) is performed during various arthroscopic shoulder surgeries to prevent postoperative impingement of the rotator cuff [10,21-23] and to ensure a sufficient surgical view of the subacromial space.[25] Although the rate of complications associated with ASD is relatively low, the incidence of some complications, such as acromial fracture,[19,25,27] severe hematoma,[19] and partial deltoid detachment,[4,6,12] is nonnegligible. Moreover, the release of the coracoacromial ligament (CAL) has been reported to damage the integrity of the overlying deltoid muscle fascia[13] and induce glenohumeral instability.[9,13,18,29] An improved understanding of the morphologic features underneath the acromion and the structures attaching to the acromion is needed to prevent the incidence of complications after ASD.

Data from studies by Ogata and Uhthoff[21] and Edelson and Luchs[8] have suggested that the morphology of the undersurface of the anterolateral acromion may affect the attachment of the CAL; however, the following topics are

The Orthopaedic Journal of Sports Medicine, 9(1), 2325967120977485
DOI: 10.1177/2325967120977485

still controversial. First, the morphology of the inferior aspect of the acromion has not been clearly defined in other studies or in anatomy textbooks. Second, no study has precisely confirmed the correlation between the bony landmark and the ligamentous attachment because the bony surface of the ligamentous attachment could become disfigured when the ligaments are detached from their attachments by use of scalpels. Third, the studies by Ogata and Uhthoff and Edelson and Luchs included only older-aged cadavers and dried bones, and these anatomic findings might not reflect the morphologic features of younger and healthy specimens.

The first aim of the present study was to perform an anatomic cadaveric analysis of surrounding structures including the CAL and deltoid muscle fascia on the acromial morphology. The second aim was to analyze the data in living middle-aged patients with asymptomatic shoulders and thus verify the structural data obtained from the cadavers. Our first hypothesis was that the location of the bony morphology would correspond to the attachments of the CAL. The second hypothesis was that the CAL would be continuous to the deep layer of the deltoid middle head in the lateral acromion. The third hypothesis was that similar bony morphologic features would be detected in both cadaveric shoulders and asymptomatic shoulders of middle-aged patients. The third hypothesis was made because previous studies using cadavers and dried bones may not have reflected the morphological features of younger and healthy specimens.[8,21]

METHODS

The protocols for both arms of this study received approval from institutional review boards and the patients provided informed consent.

Cadaveric Study of the Relationship Between Acromial Morphology and CAL

Between January 2018 and July 2018, a total of 28 shoulders (14 right, 14 left) from 14 Japanese cadavers (6 male, 8 female) were examined at Tokyo Medical and Dental University. We used 4 shoulders (2 right, 2 left) for the pilot study and assigned 24 shoulders (12 right, 12 left) from 14 cadavers to the current study. All cadavers were donated to the Department of Anatomy of our institution for education and study. During dissection, RCTs (2 bursal-side partial tears, 4 full-thickness tears) were seen in 6 shoulders (3 right, 3 left) from 4 cadavers (all female), which were excluded from this study because of the possible deformity of the acromion. No shoulders had severe deformity of the acromion or past history of shoulder surgery. As a result, we analyzed 18 shoulders (9 right, 9 left) from 11 cadavers (6 male, 5 female). The mean age of the specimens was 79.8 years (range, 70-103 years).

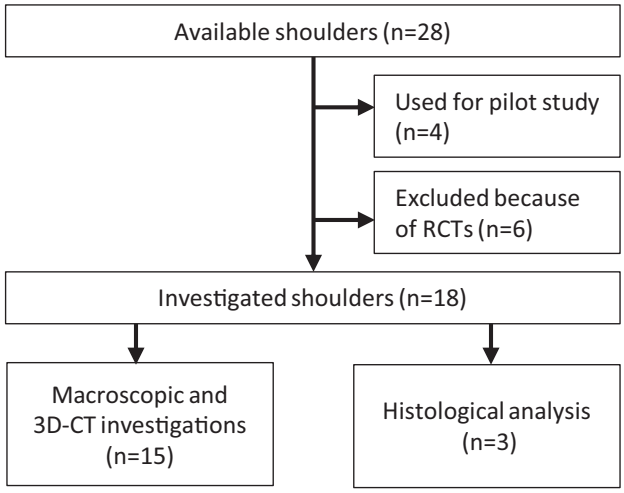

Figure 1. Flow diagram of the study enrollment process. RCT, rotator cuff tear; 3D-CT, 3-dimensional computed tomography.

All cadavers were fixed in 8% formalin and preserved in 30% ethanol. Each shoulder was obtained by sectioning at the middle of the humerus and the clavicle. After removing the skin and subcutaneous tissues from the shoulder, we removed the head of the humerus and glenoid of the scapula. A total of 15 shoulders from 9 cadavers (5 male, 4 female) were subjected to both macroscopic and 3-dimensional computed tomography (3D-CT) investigations (7 right, 8 left), and the remaining 3 shoulders from 3 cadavers (2 males, 1 female) were selected at random for the histologic analysis (Figure 1).

3D-CT Measurement. After we observed the 15 cadaveric shoulders with the deltoid attached (Figure 2A), the deltoid was detached from the clavicle and reflected laterally (Figure 2B). Next, we removed the soft tissue below the deltoid to investigate the CAL and surrounding structures. The CAL was identified as the thick part of the

§Address correspondence to Akimoto Nimura, MD, PhD, Department of Functional Joint Anatomy, Graduate School of Medical and Dental Sciences, Tokyo Medical and Dental University, 1-5-45 Yushima, Bunkyo-ku, Tokyo 113-8519 Japan (email: nimura.orj@tmd.ac.jp).
*Department of Clinical Anatomy, Graduate School of Medical and Dental Science, Tokyo Medical and Dental University, Tokyo, Japan.
†Funabashi Orthopaedic Sports Medicine and Joint Center, Funabashi, Chiba, Japan.
‡Department of Functional Joint Anatomy, Graduate School of Medical and Dental Sciences, Tokyo Medical and Dental University, Tokyo, Japan.
‖Tokyo Sports and Orthopaedic Clinic, Tokyo, Japan.
Final revision submitted June 27, 2020; accepted August 5, 2020.
One or more of the authors has declared the following potential conflict of interest or source of funding: This study was partly supported by a Grant-in-Aid for Scientific Research from the Ministry of Education, Culture, Sports(C) (No. 16K10890) and by a grant from JA Kyosai Research Institute (Agricultural Cooperative Insurance Research Institute). AOSSM checks author disclosures against the Open Payments Database (OPD). AOSSM has not conducted an independent investigation on the OPD and disclaims any liability or responsibility relating thereto.
Ethical approval for this study was obtained from Tokyo Medical and Dental University for the cadaveric study (protocol No. M2018-304) and Funabashi Orthopaedic Hospital for the study with living patients (ID No. 2018002).

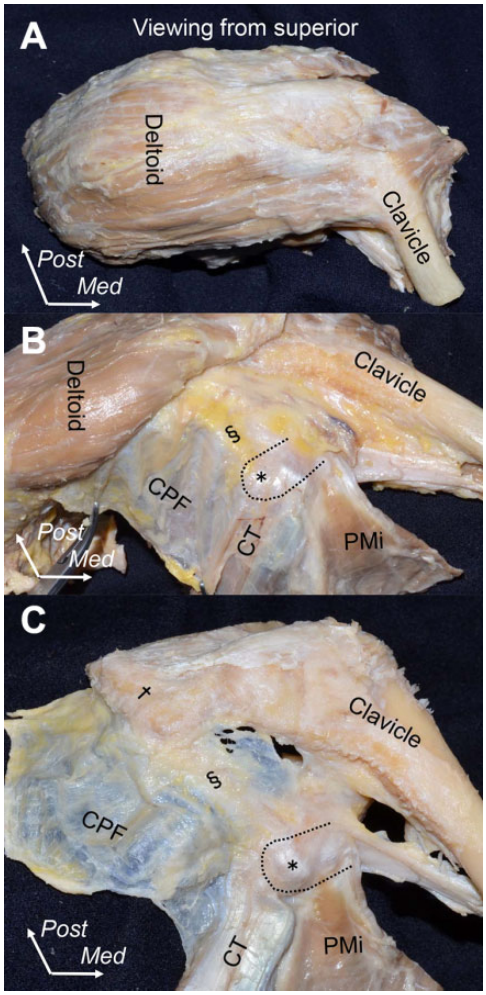

Figure 2. Dissection of the clavipectoral fascia and coracoacromial ligament from the superior aspect. (A) Superior aspect of the deltoid muscle and clavicle after removal of skin and subcutaneous tissues. (B) The coracoacromial ligament (§) and clavipectoral fascia were observed after detachment of the deltoid muscle from the clavicle and lateral reflection. (C) The coracoacromial ligament (§) appears as a thick part of the clavipectoral fascia after removal of the deltoid muscle from the acromion (†) and the synovial tissue above the coracoacromial ligament. The black dotted area and asterisk in (B) and (C) mark the coracoid process. CPF, clavipectoral fascia; CT, conjoint tendon; Med, medial; PMi, pectoralis minor; Post, posterior.

clavipectoral fascia between the acromion and the coracoid process (Figure 2C). Next, we investigated the inferior aspect of the acromion to clarify the attachment of the CAL to the acromion (Figure 3).

The CAL attachment and anterolateral prominence were examined on micro 3D-CT images (inspeXio SMX-100CT; Shimadzu) using application software (VGStudio Max 2.0). A single surgeon (Y.U.) performed all measurements of the anterolateral prominence in the cadavers and in living middle-aged patients with asymptomatic shoulders using Geomagic Studio software (3D Systems). The prominence underneath the anterolateral acromion was observed, and the maximum length was measurable from the anteromedial to posterolateral direction in all cases. First, the dimensions of the anterolateral prominence were measured using 3D-CT without markers. The long axis was defined as the maximum length from the anteromedial direction near the acromioclavicular joint to the posterolateral direction of the prominence (Figure 4A). The width was defined as the widest line perpendicular to the long axis (Figure 4A). The virtual plane was defined by 3 random points in the flat area posterior to the anterolateral prominence of the acromion. The height was defined as the length of a perpendicular line from the virtual plane to the most inferior point of the anterior acromion (Figure 4, B and C). Second, the relationship between the prominence and the CAL was examined using 3D-CT with radiopaque markers. The radiopaque markers (1 mm^2), which were made by cutting an angioplasty catheter into 1-mm^2 pieces, were placed at 5-mm intervals along the posterior border of the CAL. The acromial types were classified using the classification by Bigliani et al[2] (flat type, curved type, and hooked type) on outlet view of 3D-CT images.

Before making the measurements, we hypothesized that the sizes of the long axis, width, and height would have no significant differences between the 2 groups. We reached a consensus to use the respective minimum values of 2 mm, 1.5 mm, and 1.5 mm for the sample size calculation of our study because no previous study has clearly identified minimally important differences. Using a type I error rate of 5% and power of 80%, we calculated that a minimum of 15 patients would be required in each group. For power analysis, we used SDs of 2 mm, 1.5 mm, and 1.5 mm for the long axis, width, and height, respectively, in the preliminary data.

Histologic Analysis. Two of the authors (A.N. and Y.U.) performed histologic analysis of the cadavers. A total of 3 shoulders from 3 cadavers were subjected to histologic analysis. We sectioned each acromion en bloc at the oblique coronal plane and perpendicular to the lateral edge of the acromion using a diamond-band pathology saw (Exakt 312; Exakt Advanced Technologies GmbH). Blocks were dehydrated for 1 week in a solution containing chloride, hydrochloric acid, and formic acid, as described by Plank and Rychlo.[26] After dehydration of the tissue blocks, we embedded them in paraffin and cut serial sections (5 μm thick) parallel to the sectioned plane. The sections were stained using Masson trichrome to visualize the collagen tissue in the coracoacromial ligament and the deltoid fascia as a densely stained area.

Comparison of Measurements in Living Patients Using 3D-CT Imaging

To verify the cadaveric data, we evaluated 3D-CT scans of the asymptomatic shoulders of living middle-aged patients by use of a 16-detector CT system (Alexion; Toshiba) (image matrix, 512 × 512; pixel size, 0.468 × 10.468 mm; slice

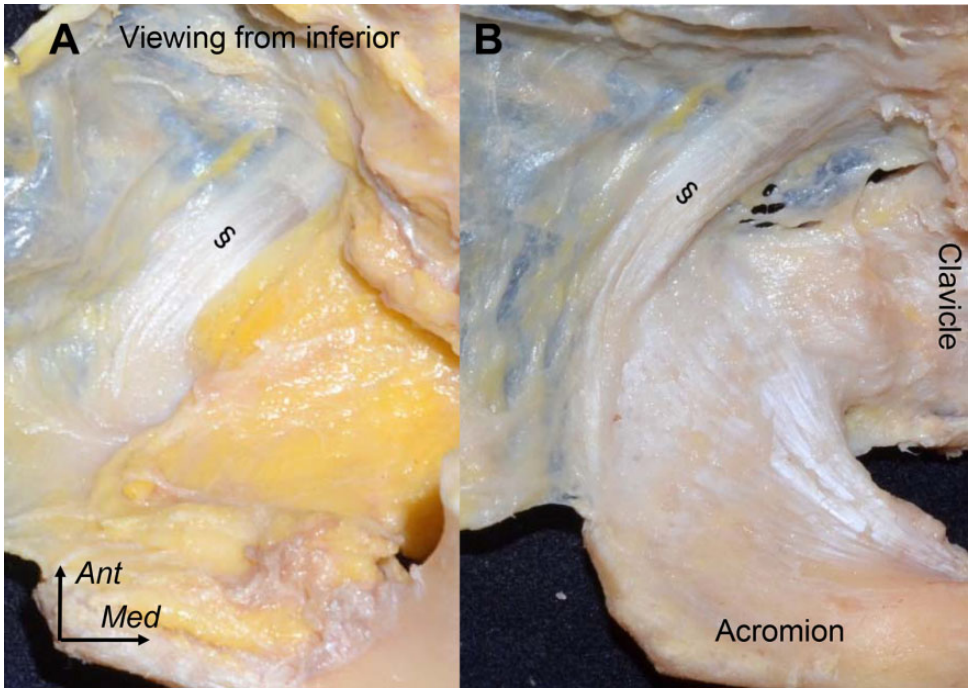

Figure 3. Dissection of the attachment of the coracoacromial ligament and medial border of the anterolateral prominence from the inferior aspect. (A) The coracoacromial ligament (§) and synovial tissue were observed in the inferior view after removal of the humeral head and glenoid in the same case shown in Figure 2. (B) The coracoacromial ligament (§) and distal clavicle were observed after removal of the synovial tissue. Ant, anterior; Med, medial.

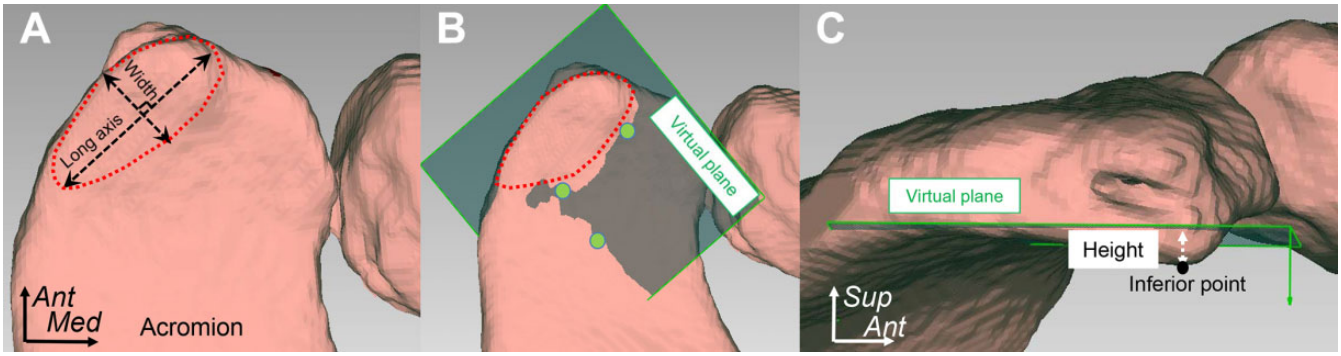

Figure 4. Measurement of the anterolateral acromial prominence. (A) The long axis was measured from the anteromedial to the posterolateral direction, and the width was measured as a line perpendicular to the long axis. (B, C) The height was measured from a virtual plane formed by 3 random points (green circles) on the flat area of the acromion to the most inferior point of the acromion. Ant, anterior; Med, medial; Sup, superior.

pitch, 0.3 mm). This system allowed bilateral shoulder imaging without an increased radiation dose.

Between January 2018 and July 2018, patients aged 50 to 59 years who visited Funabashi Orthopaedic Sports Medicine and Joint Center for the treatment of shoulder instability were consecutively recruited so we could study the asymptomatic shoulders of living middle-aged patients. From our large cohort of patients with shoulder instability, we enrolled 24 consecutive patients with asymptomatic shoulders contralateral to the unstable shoulders (16 male patients, 8 female patients; 10 right shoulders, 14 left shoulders; mean age, 54.8 years; age range, 52-59 years). We obtained bilateral shoulder CT images of patients with unilateral shoulder instability. After CT imaging, the humeral head was digitally subtracted from images of the acromion using ITK-SNAP software (Version 3.6.0; Penn Image Computing and Science Lab5 T). We measured the dimensions of the anterolateral prominence including the long axis, width, and height, and the acromial type was classified as described for cadavers.

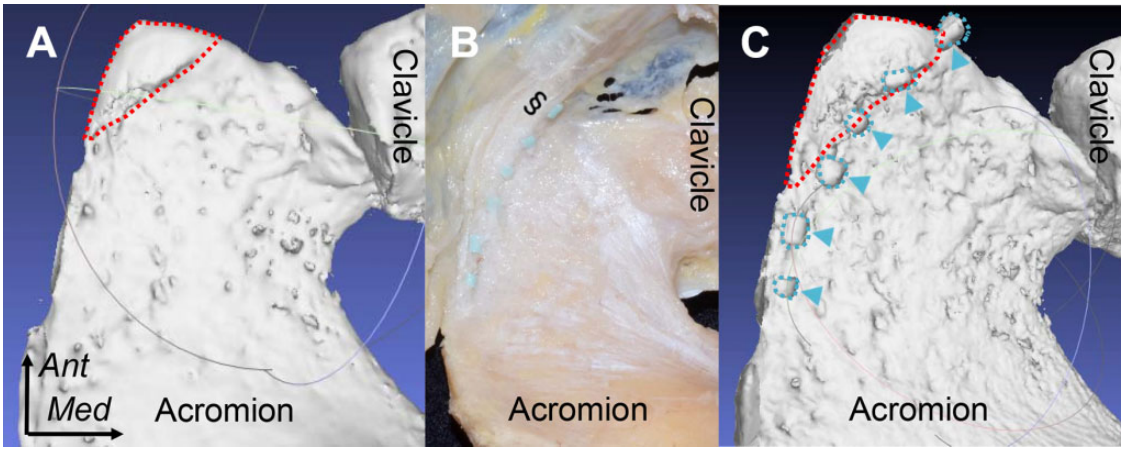

Figure 5. (A) Location of the prominence at the anterolateral acromion (red dotted area), which has a posterior margin from the anteromedial corner of the acromion near the acromioclavicular joint to the lateral edge of the acromion with the posterior curve. (B) Placement of radiopaque markers at the medial border of the coracoacromial ligament. (C) Plain 3-dimensional computed tomography image showing correspondence between the markers (blue arrows) and the medial border of the anterolateral prominence of the acromion (red dotted area). Ant, anterior; Med, medial.

Statistical Analysis

An unpaired *t* test was used to compare continuous data between the cadaveric specimens and asymptomatic shoulders of living middle-aged patients. The Fisher exact test for count data was used to compare the Bigliani classification between cadaveric specimens and asymptomatic shoulders. Statistical analyses were conducted using R Version 3.1.0 (R Foundation for Statistical Computing). The level of significance was set at $P < .05$.

To investigate the intra- and interobserver variability of the measurements in the asymptomatic shoulders, we used models from 20 randomly selected patients. To evaluate intraobserver variability, a single surgeon (Y.U.) measured all patients 3 times at 1-week intervals. The intraclass correlation coefficient (ICC) was determined for each parameter. To evaluate interobserver variability, 2 surgeons (Y.U. and K.M.) independently measured the images, and the ICC was determined for each parameter.

RESULTS

For the comparison of 3D-CT measurements, the 15 cadaveric specimens were significantly older than the 24 middle-aged patients: the mean ± SD age was 79.8 ± 1.5 versus 54.8 ± 2.5 years, respectively ($P < .001$). We found no difference in the sex distribution between groups (cadaveric specimens, 8 male and 7 female shoulders; middle-aged patients, 16 male and 8 female shoulders; $P = .693$).

Results of the Cadaveric Study

After removing the skin and subcutaneous tissues (Figure 2A) and detaching and reflecting the deltoid, we observed integration of the clavipectoral fascia with the deep fascia of the deltoid muscle (Figure 2B). The superficial layer of the conjoint tendon and pectoralis minor muscle appeared in the same layer as the CAL and clavipectoral fascia (Figure 2C). Observation of the acromion in the inferior view revealed that the CAL and synovial tissues covered this structure (Figure 3A). Removal of these tissues revealed that the CAL was attached to the coracoid process and lateral edge of the acromion (Figure 3B).

TABLE 1
3-Dimensional Computed Tomography Measurements of the Bony Prominence[a]

Measurement	Cadaveric Specimens (n = 15)	Asymptomatic Shoulders of Middle-Aged Patients (n = 24)	*P* Value
Long axis	18.7 ± 2.1	19.2 ± 3.0	.515
Width	7.0 ± 1.7	6.3 ± 1.4	.091
Height	2.3 ± 1.2	2.8 ± 1.4	.411

[a]Data are reported in millimeters as mean ± SD.

Results of 3D-CT Measurement. Micro 3D-CT imaging demonstrated agreement between the locations of the radiopaque markers and the medial border of the anterolateral prominence of the acromion in all cases (Figure 5). In all cadavers, 3D-CT imaging revealed a prominence below the acromion, with a measurable long axis, width, and height (Table 1). The prominence was located at the anterolateral acromion, for which the posterior margin extended from the anteromedial corner of the acromion near the acromioclavicular joint to the lateral edge of the acromion with the posterior curve in all shoulders (Figure 5). All the cadaveric specimens were classified as having curved-type acromion on outlet view of 3D-CT images (Figure 7).

Results of Histologic Analysis. Histologic analyses revealed that the CAL fiber was attached from the medial border of the bony prominence to the lateral edge of the

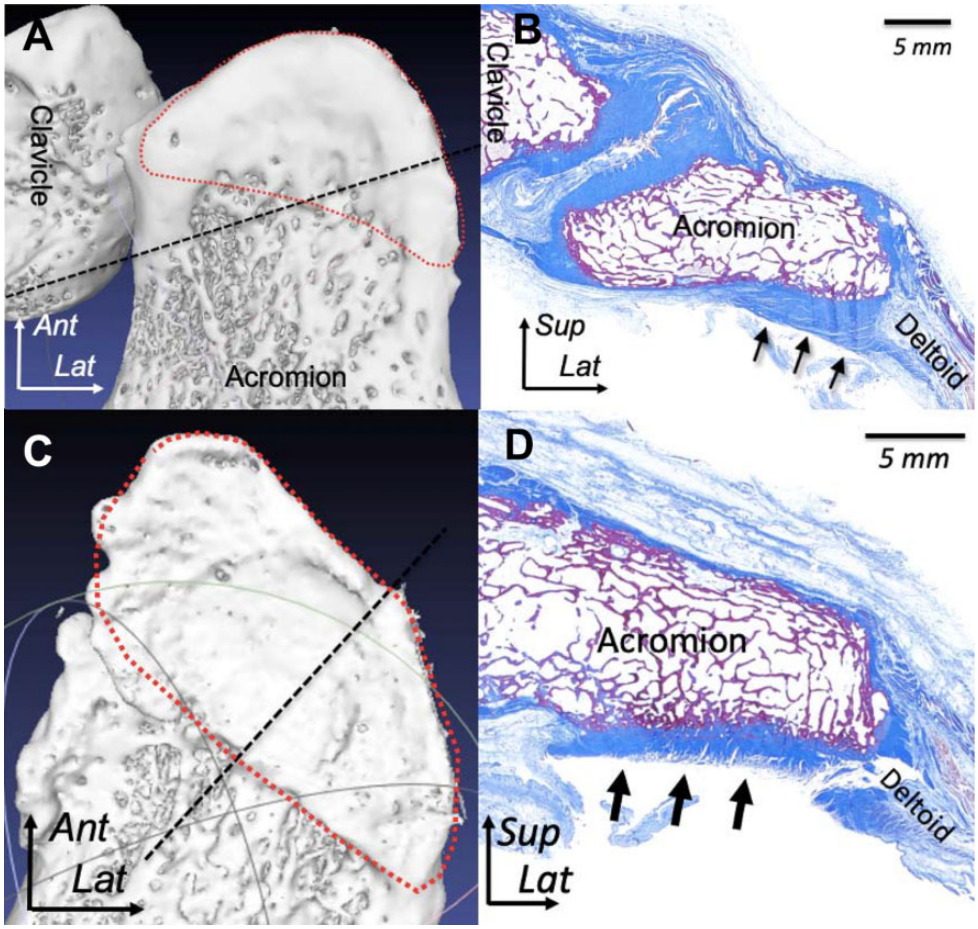

Figure 6. Histologic analysis of the coracoacromial ligament below the acromion. Two sections from 2 different specimens are shown. (A, C) The sectioning lines are shown as black dotted lines across the anterolateral acromial prominences (red dotted area). (B, D) The coracoacromial ligaments (black arrows) are observed below the acromion. Ant, anterior; Lat, lateral; Sup, superior.

acromion and was stained strongly with Masson trichrome. The origins of the deltoid middle head were observed at the lateral edge of the acromion. The CAL was continuous to the deep layer and the deep fascia of the deltoid middle head (Figure 6).

Comparison With Living Patients

In all asymptomatic shoulders in middle-aged patients, 3D-CT imaging revealed a prominence below the acromion, with a measurable long axis, width, and height (Table 1). These dimensions did not differ significantly between the cadaveric specimens and asymptomatic shoulders of living middle-aged patients (long axis, $P = .515$; width, $P = .091$; height, $P = .411$) (Table 1, Figure 8). All the shoulders except 1 were classified as curved type. One shoulder was classified as having hooked-type acromion (Figure 7).

Intra- and Interobserver Variability. High intraobserver variability was observed for each parameter (ICC = 0.92 for long axis, 0.96 for width, 0.92 for height, and 1.00 for acromial type). Similarly, high interobserver variability of 2 surgeons (Y.U., K.M.) was observed for each parameter (ICC = 0.93 for long axis, 0.92 for width, 0.91 for height, and 1.00 for acromial type).

DISCUSSION

This study revealed a correlation between the attachment site of the CAL underneath the acromion and the presence of the anterolateral acromial prominence. Moreover, the CAL was continuous the middle head of the deltoid muscle at the lateral acromion. Notably, this anterolateral acromial prominence was observed in all cadaveric specimens and asymptomatic shoulders of middle-aged patients.

Neer[20] first reported the presence of the anterior prominence below the acromion in elderly patients. Ogata and Uhthoff[21] reported the correspondence of the acromial prominence and insertion of the CAL underneath the anterior acromion in a histologic analysis. Edelson and Luchs[8] reported that enthesopathic bony transformation of the CAL was observed below the acromion in dry bones, which corresponded to the insertion of CAL underneath the anterior acromion in cadavers. In contrast, previous studies on CAL have not mentioned the attachment of CAL

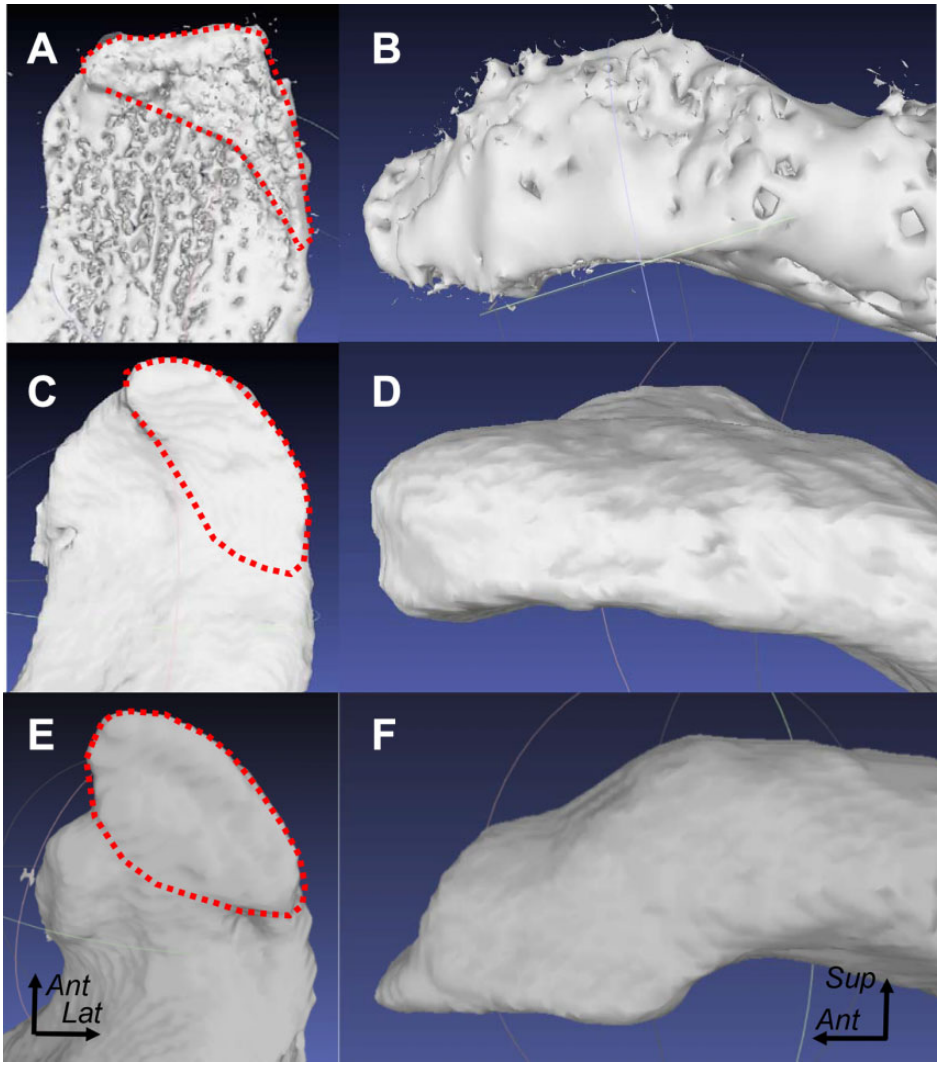

Figure 7. The classification of acromion type according to Bigliani et al.[2] (A) The inferior aspect of the acromion of a cadaver. (B) The acromion was of the curved type in the case of (A) in the lateral view. (C, E) The inferior aspects of the acromion in asymptomatic shoulders of middle-aged patients. (D) The acromion was the curved type in the case of (C). (F) The acromion was the hooked type in the case of (E). Red dotted area marks the anterolateral prominence. Ant, anterior; Med, medial; Sup, superior.

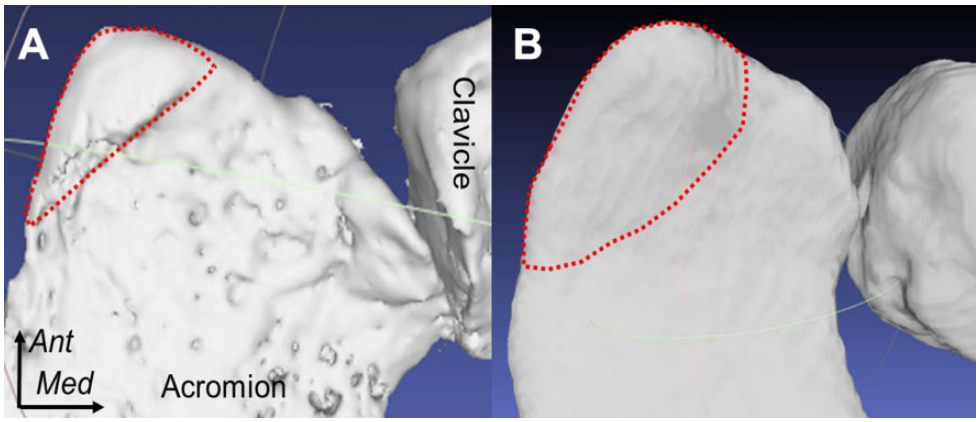

Figure 8. Anterolateral prominence below the acromion. The prominence (red dotted line) was located in the anterolateral acromion in both (A) older-aged cadavers and (B) living middle-aged patients with asymptomatic shoulders. Ant, anterior; Med, medial.

underneath the acromion,[1,3,5,15] and in anatomy textbooks, the native structure of the acromion is assumed to include a flat-shaped undersurface.[7,11] Based on the results of our study, however, the undersurface of the acromion is not flat; rather, an anterolateral acromial prominence was detected in all cadaveric specimens and asymptomatic shoulders of living middle-aged patients. Based on our study, this prominence appears to be a native structural feature underneath the acromion. Moreover, most of the acromia in older-aged cadavers and asymptomatic shoulders of living middle-aged patients in this study were classified as curved type, which supported the result of this study that the anterolateral acromial prominence underneath the acromion was a native structure.

Based on their histologic analyses, Ogata and Uhthoff[21] reported that the anterior prominence corresponded to the area covered by the CAL on the undersurface of the acromion. Edelson and Luchs[8] similarly reported this correspondence based on studies of cadavers and dry bones. However, neither previous study involved dissection of the CAL attachment, and therefore the anatomic correspondence of these structures could not be depicted accurately without artifacts caused by the dissection of soft tissues using scalpels. Our study evaluated cadaveric specimens using 3D-CT and radiopaque markers and demonstrated a precise correspondence between the acromial prominence and the site of CAL attachment.

Anatomy textbooks and previous papers have described the middle head of the deltoid muscle as the most reliable part of that muscle and have reported the presence of many intramuscular tendons that attach to the lateral acromion.[7,11,17,28] However, anatomy reports of the relationship between the CAL and deltoid muscle have been conducted in the anterior acromion.[8,14,21] Only Torpey et al[30] quantitatively investigated the attachment to the lateral acromion; however, the soft tissue evaluation was not included. The histologic evaluation in this study revealed that the CAL partly formed the middle head of the deltoid muscle in the lateral acromion. In other words, resection of the anterolateral prominence and the CAL underneath the acromion could compromise the deltoid attachment to the lateral acromion.

Previous studies have suggested that an anterolateral prominence underneath the acromion might develop as a result of ossification induced by RCT-mediated impingement of the acromion because of RCTs[16] or shear stress due to an attachment of the CAL underneath the acromion.[24] Moreover, direct contact pressure from the humeral head may affect development of the anterolateral prominence.[31] Our study revealed that the anterolateral prominence underneath the acromion may be a native structure. Furthermore, this prominence corresponds to the attachment of the CAL, which partially forms the origin of the middle head of the deltoid muscle. Regardless of the mechanism that leads to the morphologic dimensions of the acromion in the inferior aspect including the long axis, width, and height, the attachment of the CAL is clearly associated with this prominence.

Our study findings may be clinically relevant with regard to the surgical indication for ASD. We suggest that complications of ASD, such as deltoid detachment, could be prevented by minimizing damage to the CAL and the origin of the middle head of the deltoid. Although Hunt et al[14] and Torpey et al[30] simulated ASD in cadavers, the safety of ASD for the deltoid muscle is still controversial regarding simulation in cadavers. Further case-control studies on the integrity and function of the deltoid muscle in living patients who have undergone ASD could contribute to the development of therapeutic strategies for arthroscopic shoulder surgeries.

This study has notable limitations. First, the relationship between the anterolateral prominence underneath the acromion and the surrounding structures was investigated only in cadaveric specimens. Although the anterolateral prominence underneath the acromion was also observed in asymptomatic shoulders of living middle-aged patients, we cannot guarantee the existence of a relationship between the anterolateral prominence underneath the acromion and the attachments of the CAL and middle head of the deltoid in living participants. Second, this is a descriptive study without clinical data, complications, or interventions; therefore, we cannot comment on the pathology of the acromial spur. Third, we did not quantitively measure the CAL attachment to the undersurface of the acromion and the origin of the deltoid middle head in the lateral acromion, which may help clinicians to determine the degree of subacromial decompression. Fourth, the number of available specimens and the histologic analysis were limited. Fifth, we did not use magnetic resonance imaging to evaluate RCTs in asymptomatic shoulders of middle-aged patients. Sixth, this study included only an Asian population; therefore, we cannot guarantee the applicability of the results to other populations.

CONCLUSION

The anterolateral prominence, which corresponds to the attachment of the CAL below the acromion, may be a native structure below the acromion. Moreover, the CAL is continuous to the deep layer of the deltoid middle head in the lateral acromion.

REFERENCES

1. Alraddadi A, Alashkham A, Lamb C, Soames R. Variability in attachment of the coracoacromial ligament in relation with its morphology. *Surg Radiol Anat*. 2017;39(12):1323-1330.
2. Bigliani LU, Morrison DS, April EW. The morphology of the acromion and its relationship to rotator cuff tears. *Orthop Trans*. 1986;10:228.
3. Balke M, Schmidt C, Dedy N, Banerjee M, Bouillon B, Liem D. Correlation of acromial morphology with impingement syndrome and rotator cuff tears. *Acta Orthop*. 2013;84(2):178-183.
4. Bonsell S. Detached deltoid during arthroscopic subacromial decompression. *Arthroscopy*. 2000;16(7):745-748.
5. Chahla J, Marchetti DC, Moatshe G, et al. Quantitative assessment of the coracoacromial and the coracoclavicular ligaments with 3-dimensional mapping of the coracoid process anatomy: a cadaveric study of surgically relevant structures. *Arthroscopy*. 2018;34(5):1403-1411.

6. Cho NS, Cha SW, Rhee YG. Alterations of the deltoid muscle after open versus arthroscopic rotator cuff repair. *Am J Sports Med*. 2015; 43(12):2927-2934.
7. Clemente C. Osteology, and muscles and fasciae of the upper limb. In: Clemente C, ed. *Gray's Anatomy 30th American Edition*. Lea & Febiger; 1985:233-234.
8. Edelson JG, Luchs J. Aspects of coracoacromial ligament anatomy of interest to the arthroscopic surgeon. *Arthroscopy*. 1995;11(6): 715-729.
9. Fagelman M, Sartori M, Freedman KB, Patwardhan AG, Carandang G, Marra G. Biomechanics of coracoacromial arch modification. *J Shoulder Elbow Surg*. 2007;16(1):101-106.
10. Fujisawa Y, Mihata T, Murase T, Sugamoto K, Neo M. Three-dimensional analysis of acromial morphologic characteristics in patients with and without rotator cuff tears using a reconstructed computed tomography model. *Am J Sports Med*. 2014;42(11): 2621-2626.
11. Gray H, Pick T, Howden R, eds. *Gray's Anatomy*. 15th ed. Lea Brothers; 1901.
12. Groh GI, Simoni M, Rolla P, Rockwood CA. Loss of the deltoid after shoulder operations: an operative disaster. *J Shoulder Elbow Surg*. 1994;3(4):243-253.
13. Hansen U, Levy O, Even T, Copeland SA. Mechanical properties of regenerated coracoacromial ligament after subacromial decompression. *J Shoulder Elbow Surg*. 2004;13(1):51-56.
14. Hunt JL, Moore RJ, Krishnan J. The fate of the coracoacromial ligament in arthroscopic acromioplasty: an anatomical study. *J Shoulder Elbow Surg*. 2000;9(6):491-494.
15. Kesmezacar H, Akgun I, Ogut T, Gokay S, Uzun I. The coracoacromial ligament: the morphology and relation to rotator cuff pathology. *J Shoulder Elbow Surg*. 2008;17(1):182-188.
16. Kim YS, Bigliani LU, Fujisawa M, et al. Stromal cell-derived factor 1 (SDF-1, CXCL12) is increased in subacromial bursitis and downregulated by steroid and nonsteroidal anti-inflammatory agents. *J Orthop Res*. 2006;24(8):1756-1764.
17. Kumar VP, Satku K, Liu J, Shen Y. The anatomy of the anterior origin of the deltoid. *J Bone Joint Surg Br*. 1997;79(4):680-683.
18. Lee TQ, Black AD, Tibone JE, McMahon PJ. Release of the coracoacromial ligament can lead to glenohumeral laxity: a biomechanical study. *J Shoulder Elbow Surg*. 2001;10(1):68-72.
19. Matthews LS, Burkhead WZ, Gordon S, Racanelli J, Ruland L. Acromial fracture: a complication of arthroscopic subacromial decompression. *J Shoulder Elbow Surg*. 1994;3(4):256-261.
20. Neer CS II. Anterior acromioplasty for the chronic impingement syndrome in the shoulder: a preliminary report. *J Bone Joint Surg Am*. 1972;54(1):41-50.
21. Ogata S, Uhthoff HK. Acromial enthesopathy and rotator cuff tear: a radiologic and histologic postmortem investigation of the coracoacromial arch. *Clin Orthop Relat Res*. 1990;254:39-48.
22. Ogawa K, Yoshida A, Inokuchi W, Naniwa T. Acromial spur: relationship to aging and morphologic changes in the rotator cuff. *J Shoulder Elbow Surg*. 2005;14(6):591-598.
23. Oh JH, Kim JY, Lee HK, Choi JA. Classification and clinical significance of acromial spur in rotator cuff tear: heel-type spur and rotator cuff tear. *Clin Orthop Relat Res*. 2010;468(6):1542-1550.
24. Park I, Lee HJ, Kim SE, Bae SH, Byun CH, Kim YS. Which shoulder motions cause subacromial impingement? Evaluating the vertical displacement and peak strain of the coracoacromial ligament by ultrasound speckle tracking imaging. *J Shoulder Elbow Surg*. 2015;24(11): 1801-1808.
25. Paulos LE, Franklin JL. Arthroscopic shoulder decompression development and application: a five year experience. *Am J Sports Med*. 1990;18(3):235-244.
26. Plank J, Rychlo A. A method for quick decalcification. Article in undetermined language. *Zentralbl Allg Pathol*. 1952;89(8):252-254.
27. Rupp S, Seil R, Kohn DM. Surgical reconstruction of a stress fracture of the acromion after arthroscopic subacromial decompression in an elite tennis player. *Arthroscopy*. 1998;14(1):106-108.
28. Sakoma Y, Sano H, Shinozaki N, et al. Anatomical and functional segments of the deltoid muscle. *J Anat*. 2011;218(2):185-190.
29. Su WR, Budoff JE, Luo ZP. The effect of coracoacromial ligament excision and acromioplasty on superior and anterosuperior glenohumeral stability. *Arthroscopy*. 2009;25(1):13-18.
30. Torpey BM, Ikeda K, Weng K, van der Heeden D, Chao EY, McFarland EG. The deltoid muscle origin: histologic characteristics and effects of subacromial decompression. *Am J Sports Med*. 1998;26(3):379-383.
31. Yamamoto N, Muraki T, Sperling JW, et al. Contact between the coracoacromial arch and the rotator cuff tendons in nonpathologic situations: a cadaveric study. *J Shoulder Elbow Surg*. 2010;19(5): 681-687.